Guide-directed DNA cleavage by a prokaryotic Argonaute protein induces chromosome recombination in *Escherichia coli*

Authors: Shan Huang[1]*, Kaihang Wang[2]*, Stephen L. Mayo[1, 2]*

Affiliations:

[1]Division of Chemistry and Chemical Engineering, California Institute of Technology, MC 114-96, 1200 East California Boulevard, Pasadena, CA 91125, USA.

[2]Divisions of Biology and Biological Engineering, California Institute of Technology, MC 147-75, 1200 East California Boulevard, Pasadena, CA 91125, USA

*Corresponding author. Email: gibbson783@gmail.com (S.H.); kaihangwang@caltech.edu (K.W.); smayo@caltech.edu (S.L.M.)

Abstract: Emerging evidence supports the argument that some prokaryotic argonautes (pAgos) serve as a defensive system against the invasion of viruses and plasmids through guide DNAs (gDNAs) directed DNA cleavage. This DNA-guided DNA interference motivates research to induce genomic mutations via pAgo mediated cleavage. Here we demonstrate that CbAgo, a pAgo from *Clostridium butyricum*, is able to induce chromosomal recombination between direct repeat sequences via its gDNA-directed cleavage in *Escherichia coli* chromosomes. We also show that CbAgo targeting can assist Lambda-Red recombineering in RecA-deficient strain. Our study reveals that cleavage by CbAgo in *E. coli* chromosomes can be mutagenic and suggests its broader application in genetic manipulation.

One-Sentence Summary: Prokaryotic argonaute induces chromosome recombination in *Escherichia coli* via guide DNA-directed cleavage.

Main Text:

Prokaryotic argonaute proteins (pAgos) constitute a diverse protein family (*1-2*). Unlike their eukaryotic counterparts, which use small RNA guides to interfere with RNA targets in regulation and defense (*3-4*), many pAgos were reported to cleave DNA targets using small guide DNAs (gDNAs) *in vitro* (*5-18*). *In vivo*, several pAgos were shown to protect bacteria from foreign DNAs (*7, 19-20*), but the defense mechanism, especially whether double-stranded DNA breaks (DSBs) are involved, remained elusive until recently. In-depth insights into the mechanism of pAgo-mediated defense were gained by analyzing CbAgo, a pAgo nuclease from a mesophilic bacterium *Clostridium butyricum*, in *Escherichia coli* as its expression host (*21*). In that study, a DNA interference pathway was revealed in CbAgo-mediated protection against invading DNAs. First, CbAgo generates and binds small gDNAs from plasmids or other multicopy genetic elements. Next, gDNA-bound CbAgo introduces DSBs at the target sites, including chromosomal regions, and causes DNA degradation in collaboration with *E. coli* exonuclease RecBCD. Such a mechanism enables the host cell to defend invader DNAs such as plasmids and phages.

The observation that CbAgo can be directed to generate DSBs in chromosomes by plasmid-encoded guide sequences (GSs) motivated us to leverage such a mechanism to manipulate the *E. coli* genome, reasoning DSB generation is the essential step to introduce mutations by genome editing systems such as CRISPR/cas9, TALEN, Zinc-finger nucleases (*22-26*). Until now, mutations induced by guide-directed cleavage of CbAgo or other pAgos in the host genome have never been established.

Here we demonstrate that CbAgo, directed by GSs on plasmids, is able to induce chromosome recombination between direct repeat sequences in *E. coli*. This recombination system requires both guide and CbAgo cleavage activity. We further show that (a) CbAgo-GS

induces *E. coli* SOS response, and (b) RecBCD, the exonuclease from *E. coli* cellular DNA repair machinery (*27-28*), plays an essential role in the recombination by CbAgo-GS, confirming the DSB generation during recombination. Besides, such DSBs introduced by guide-directed CbAgo cleavage cause severe growth inhibition in RecA-deficient *E. coli* strain, which can be utilized as counter-selection to assist Lambda-Red recombineering. These findings demonstrate the potential of establishing a DNA-directed genome editing system using pAgo.

Previous observation that guide-directed CbAgo cleavage at *E. coli* chromosome efficiently triggers RecBCD activity (*21*) inspired us to hypothesize that RecBCD-dependent chromosome recombination should be triggered by guide-directed CbAgo cleavage as well. It has been shown that DSBs introduced by SbcCD cleavage at a 246-bp chromosomal palindrome (pal246) stimulate RecBCD-dependent recombination between two downstream direct repeat sequences (*29*). To determine whether similar recombination can be induced by guide-directed CbAgo cleavage (Fig. 1A), we integrated a recombination cassette at cynX loci on *E. coli* strain DL1777, which is ~6 kb away from the target lacZ loci (Fig. 1B). This recombination cassette contains an EM7 promoter and a kanamycin resistance gene whose function is abolished by the insertion of a stop codon array and a 270-bp direct repeat sequence. A recombination event between the two direct repeat sequences removes the insertion, restores the gene function, and confers kanamycin resistance to the host. Considering the introduction of the Chi site, an 8-base 5'-GCTGGTGG-3' motif recognized by RecBCD (*27, 30-31*), has been shown to stimulate RecBCD recombination (*29*), we also incorporated a varied number of Chi sites into the genome, with their 5' ends oriented towards the recombination cassette (Fig. 1B).

To target lacZ loci, we created a targeting plasmid pTet_CbAgo-GS encoding a CbAgo expression cassette under the control of a tetracycline-inducible promoter (pTet), and a 1000-bp GS homologous to lacZ gene (Fig. 1C). Importantly, GS is the only sequence on the plasmid

(except for an 80-bp rrnB T1 terminator sequence) that is homologous to the genome, assuring only the lacZ loci will be effectively targeted. For controls, plasmids with no GS, no CbAgo gene, or neither, were created. To determine the dependence of CbAgo cleavage activity, we created plasmids encoding a CbAgo mutant (dCbAgo: CbAgo D541A-D611A) that contains mutations of two catalytic residues in its active site which were previously shown to abolish its endonuclease activity *in vitro* (*12-13*) and DSB generation activity *in vivo* (*21*).

We then combined the obtained plasmids and strains, induced CbAgo expression, and recovered induced cells to measure recombination frequencies, which was calculated as the fraction of ampicillin-resistant cells that became resistant to kanamycin (kanamycin-resistant and ampicillin-resistant colony-forming units (cfu)/ampicillin-resistant cfu), because only the recombinants have restored functional kanamycin resistance gene. When there are three or six Chi sites adjacent to the recombination cassette (corresponding strain 3×ChikanS and 6×ChikanS), recombination frequencies by CbAgo-GS are significantly higher than the rest control groups (fig. S2A), suggesting a recombination pathway that is mediated by guide-directed CbAgo cleavage.

Interestingly, we also observed remarkable recombination frequencies in dCbAgo-GS groups in some conditions (fig. S2A). When there is no Chi site adjacent to the recombination cassette (corresponding strain nonChikanS), the cell bearing dCbAgo-GS had a recombination frequency being ~tenfold higher than the one bearing CbAgo-GS. These results suggest there is a recombination pathway that is mediated by the non-cleavage function of CbAgo and is outperformed by the cleavage-dependent pathway in the presence of the CbAgo active site. Although the exact mechanism remains unknown, this dCbAgo-mediated recombination pathway should be independent of DSB and RecBCD because dCbAgo-GS was previously shown not able to generate DSB or trigger RecBCD activity *in vivo* (*21*).

We also examined the effects of GS length on the recombination frequency (fig. S2B) and found that in the range of 50 to 500 bp, recombination frequency increases as GS length increases. We decided to use 1000 bp as the GS length and 3×ChikanS as the model strain to perform fluctuation analysis to estimate recombination rates (Fig. 1D, table S4). The cell bearing CbAgo-GS had a recombination rate that is fourfold higher than the ones with dCbAgo, with and without GS, 14-fold higher than the one with CbAgo-only, and 30-fold higher over the rest control groups. The actual contribution of dCbAgo-mediated recombination to the total recombination events in 3×ChikanS/CbAgo-GS should be much smaller than one-fourth because it should be largely outperformed by the cleavage-dependent pathway as previous observation suggests. Together, these findings reveal novel chromosome recombination that is induced by guide-directed CbAgo cleavage. Its Chi site dependence implies DSB formation and RecBCD processing during recombination.

To demonstrate the reliability of our recombination system, we tested four additional pAgos in strain 3×ChikanS, including CaAgo, CdAgo, CpAgo, and IbAgo (See table S5 for the summary of pAgo used in this study). In the presence of GS, the rates of recombination induced by different pAgos correlate with the rank order of their reported *in vitro* ssDNA cleavage activity (Fig. 2A, table S6, see ref. *33*). We also tested an engineered DSB in our system by integrating a pal246 into the lacZ loci on the genome of strain 3×ChikanS and its *sbcCD* knockout mutant and measuring their recombination rates (Fig. 2B, fig. S3, table S7). The sbcCD$^+$, lacZ::pal246 strain yielded ~100-fold increase of recombination rate compared to sbcCD$^+$, lacZ$^+$ strain and *sbcCD*, lacZ::pal246 strain. The bigger fold change stimulated by SbcCD-pal246 over CbAgo-GS is consistent with the previous observation that SbcCD-pal246 is more efficient in DSB generation than CbAgo-GS *in vivo* (*21*). These findings indicate a strong

correlation between pAgo DNA cleavage activity, DSB generation efficiency, and recombination rate in our system.

To gain more insight into our recombination system, we first sought to provide direct evidence that CbAgo can be directed to attack E. coli chromosomes and cause DNA damage (Fig. 1A, steps i and ii). Since DNA damage induces the cellular SOS response, we used an E. coli strain carrying a chromosomally located gfp gene controlled by an SOS-inducible *sulA* promoter (*34*) and performed flow cytometry to quantify single-cell fluorescence level (Fig. 3A). We observed a 6-fold increase of fluorescence in cells expressing CbAgo and a 15-fold increase in cells containing CbAgo-GS, while the cells containing dCbAgo-GS exhibited no difference in cellular fluorescence compared to the cells bearing empty plasmids (Fig. 3B). The fluorescence increase in cells expressing CbAgo without GS can be explained by previous observations that CbAgo actively degrades plasmids (*21*) and plasmids degradation triggers SOS-response (*35*). Importantly, the significant increase of fluorescence in cells expressing CbAgo in the presence of GS confirms that CbAgo can be guided to attack chromosomes, while dCbAgo-GS cannot.

Then we sought to determine the involvement of *E. coli* endogenous DNA repair machinery RecA and RecBCD in the recombination by creating and testing *recA* and *recBCD* knockout mutants of strain 3×ChikanS. Since the viabilities of knockout strains varied a great deal after induction (fig. S4), we determined the fluctuation analysis is no longer suitable and decided to directly analyze recombination frequencies. In *recBCD* strain, recombination frequency by CbAgo-GS had no difference with the CbAgo-only control, representing a profound change from the result using recBCD^{+} strain (Fig. 3C), indicating CbAgo-GS induced recombination depends on RecBCD (Fig. 1A, step iii). Since RecBCD works closely with DSB (*36*), this observation also suggests DSB generation in CbAgo-GS induced recombination. An interesting discovery was that the *recBCD* strain bearing dCbAgo-GS showed ~1000-fold

decreased ampicillin-resistant cfu and only ~20-fold decreased kanamycin-resistant and ampicillin-resistant cfu compared to its RecBCD$^+$ counterpart (fig. S4). These changes resulted in increased recombination frequency (Fig. 3C), suggesting dCbAgo-mediated recombination is RecBCD-independent. Moreover, this growth inhibition was reduced by ~60-fold in the presence of the CbAgo active site, suggesting it is again outperformed or inhibited when the CbAgo active site is present.

The CbAgo-GS induced DSBs can further explain the extremely low viability of *recA* strain bearing CbAgo-GS (fig. S4): without the protection of RecA, continuously introduced DSBs trigger extensive DNA degradation by RecBCD, causing enormous loss of chromosomal DNA and subsequent cell death (*37-39*). On the other hand, these cells had a high recombination frequency close to 0.1 (Fig. 3C), indicating RecA is not essential in the recombination induced by guide-directed CbAgo cleavage even though it actively repairs DSBs generated during the process. These findings prompt us to modify our model that the final step of recombination (Fig. 1A, step iv) should be independent of RecA, reminiscent of the RecA-independent, replication arrest-induced deletion (*40-41*).

The observation that cfu of *recA* strain was reduced by three orders of magnitude when its genome is targeted by CbAgo (fig. S4) is very intriguing, as it supports a strategy to leverage CbAgo-GS targeting as counter-selection to facilitate recombineering (Fig. 4A). For comparison, a self-targeting CRISPR-Cas9 system was reported to reduce cfu by three orders of magnitude in *E. coli* (*42*). Co-expressing the CRISPR-Cas9 system to eliminate unedited cells, Lambda-Red recombineering achieved an increase of efficiency by ~10^4 fold and a 65% overall mutation rate. We sought to combine the CbAgo targeting system with Lambda-Red recombineering by introducing CbAgo expression plasmids into strain SIJ488_ΔrecA, which is RecA-deficient and has arabinose inducible Lambda-Red recombineering genes integrated into its genome. We first

performed the standard recombineering procedure with dsDNA donor encoding kanamycin resistance cassette flanked by 1000-bp homology arms to replace the genomic lacZ gene. The recombineering efficiency was 1.2×10^{-4}, calculated from the fraction of cells that became kanamycin resistant. Then we performed recombineering in CbAgo-plasmids contained cells, induced CbAgo expression, and recovered the cells to characterize the proposed counter-selection effect. The cell transformed with pTet_CbAgo-GS had a mutation efficiency of 2.3×10^{-2}, representing a ~100-fold increase of efficiency from standard recombineering (Fig. 4B). Other control groups did not yield improvement, therefore the increased proportion of edited cell population depends on guide-directed CbAgo cleavage.

Our study here demonstrates the combination of CbAgo and plasmid-encoded GS is able to induce mutations in the *E. coli* chromosome, via guide-directed CbAgo cleavage of target DNA, activation of DNA repair mechanism, and subsequent chromosome recombination. This strategy may apply to other organisms if chromosomal DSBs can be introduced and necessary cellular repair machinery can be triggered. Besides, we also demonstrate the potential of pAgo targeting to assist recombineering in RecA-deficient strains as another genome editing strategy. This method may extend to RecA-active strains, if RecA activity can be efficiently inhibited by, for example, expressing RecA inhibitor (*43*). A recent study also reported NgAgo-assisted recombineering (NgAgo, pAgo from *Natronobacterium gregoryi*), but the fold change was smaller than 2 and the enhancement of editing was not dependent on NgAgo endonuclease activity (*44*).

The mechanism of guide-directed recombination by dCbAgo in our system remains unknown, although this pathway appears to be independent of RecBCD and DSB. Since dCbAgo is able to load gDNAs from plasmids *in vivo* (*21*, fig. S1), there is a possibility that dCbAgo may play a role in target recognition and following recruitment of *E. coli* nuclease or recombinase.

This speculation is supported by findings in other pAgo researches (*45-47*) and the fact that many pAgo genes have been found associated with a variety of genes including nuclease and helicase (*1*, *19*).

Although CbAgo is among the most active pAgos identified so far (*33*), its activity is still ~10-fold lower than restriction endonucleases (*13*). Our recombination system presented here can potentially serve as a selection platform, which links pAgo cleavage to the development of antibiotic resistance. Therefore, mutants with enhanced DNA cleavage activity are likely to exhibit higher survival rates and be selected. Highly active pAgo nuclease, once obtained, should have bigger potential in DNA-guided genome engineering *in vivo* (*48*), and alternatively, may serve as a versatile restriction enzyme *in vitro* with the capability of targeting theoretically any DNA sequence using small oligos as gDNAs, providing a unique advantage over commercial ones (*49*).

References and Notes

1. D. C. Swarts, K. Makarova, Y. Wang, K. Nakanishi, R. F. Ketting, E. V. Koonin, D. J. Patel, J. van der Oost, The evolutionary journey of Argonaute proteins. *Nat Struct Mol Biol*. **21**, 743–753 (2014).

2. S. Ryazansky, A. Kulbachinskiy, A. A. Aravin, The Expanded Universe of Prokaryotic Argonaute Proteins. *mBio*. **9**, e01935-18.

3. G. Meister, Argonaute proteins: functional insights and emerging roles. *Nat Rev Genet*. **14**, 447–459 (2013).

4. D. Gebert, D. Rosenkranz, RNA-based regulation of transposon expression. *WIREs RNA*. **6**, 687–708 (2015).

5. D. C. Swarts, M. M. Jore, E. R. Westra, Y. Zhu, J. H. Janssen, A. P. Snijders, Y. Wang, D. J. Patel, J. Berenguer, S. J. J. Brouns, J. van der Oost, DNA-guided DNA interference by a prokaryotic Argonaute. *Nature*. **507**, 258–261 (2014).

6. G. Sheng, H. Zhao, J. Wang, Y. Rao, W. Tian, D. C. Swarts, J. van der Oost, D. J. Patel, Y. Wang, Structure-based cleavage mechanism of Thermus thermophilus Argonaute DNA guide strand-mediated DNA target cleavage. *PNAS*. **111**, 652–657 (2014).

7. D. C. Swarts, J. W. Hegge, I. Hinojo, M. Shiimori, M. A. Ellis, J. Dumrongkulraksa, R. M. Terns, M. P. Terns, J. van der Oost, Argonaute of the archaeon Pyrococcus furiosus is a DNA-guided nuclease that targets cognate DNA. *Nucleic Acids Research*. **43**, 5120–5129 (2015).

8. E. Kaya, K. W. Doxzen, K. R. Knoll, R. C. Wilson, S. C. Strutt, P. J. Kranzusch, J. A. Doudna, A bacterial Argonaute with noncanonical guide RNA specificity. *PNAS*. **113**, 4057–4062 (2016).

9. D. C. Swarts, M. Szczepaniak, G. Sheng, S. D. Chandradoss, Y. Zhu, E. M. Timmers, Y. Zhang, H. Zhao, J. Lou, Y. Wang, C. Joo, J. van der Oost, Autonomous Generation and Loading of DNA Guides by Bacterial Argonaute. *Molecular Cell*. **65**, 985-998.e6 (2017).

10. S. Willkomm, C. A. Oellig, A. Zander, T. Restle, R. Keegan, D. Grohmann, S. Schneider, Structural and mechanistic insights into an archaeal DNA-guided Argonaute protein. *Nat Microbiol*. **2**, 1–7 (2017).

11. A. Zander, S. Willkomm, S. Ofer, M. van Wolferen, L. Egert, S. Buchmeier, S. Stöckl, P. Tinnefeld, S. Schneider, A. Klingl, S.-V. Albers, F. Werner, D. Grohmann, Guide-independent DNA cleavage by archaeal Argonaute from Methanocaldococcus jannaschii. *Nat Microbiol*. **2**, 1–10 (2017).

12. J. W. Hegge, D. C. Swarts, S. D. Chandradoss, T. J. Cui, J. Kneppers, M. Jinek, C. Joo, J. van der Oost, DNA-guided DNA cleavage at moderate temperatures by Clostridium butyricum Argonaute. *Nucleic Acids Research*. **47**, 5809–5821 (2019).

13. A. Kuzmenko, D. Yudin, S. Ryazansky, A. Kulbachinskiy, A. A. Aravin, Programmable DNA cleavage by Ago nucleases from mesophilic bacteria Clostridium butyricum and Limnothrix rosea. *Nucleic Acids Research*. **47**, 5822–5836 (2019).

14. Y. Cao, W. Sun, J. Wang, G. Sheng, G. Xiang, T. Zhang, W. Shi, C. Li, Y. Wang, F. Zhao, H. Wang, Argonaute proteins from human gastrointestinal bacteria catalyze DNA-guided cleavage of single- and double-stranded DNA at 37 °C. *Cell Discov*. **5**, 1–4 (2019).

15. A. Olina, A. Kuzmenko, M. Ninova, A. A. Aravin, A. Kulbachinskiy, D. Esyunina, Genome-wide DNA sampling by Ago nuclease from the cyanobacterium Synechococcus elongatus. *RNA Biology*. **17**, 677–688 (2020).

16. S.-Y. Kim, Y. Jung, D. Lim, Argonaute system of Kordia jejudonensis is a heterodimeric nucleic acid-guided nuclease. *Biochemical and Biophysical Research Communications*. **525**, 755–758 (2020).

17. Y. Liu, W. Li, X. Jiang, Y. Wang, Z. Zhang, Q. Liu, R. He, Q. Chen, J. Yang, L. Wang, F. Wang, L. Ma, A programmable omnipotent Argonaute nuclease from mesophilic bacteria Kurthia massiliensis. *Nucleic Acids Research*. **49**, 1597–1608 (2021).

18. E. Kropocheva, A. Kuzmenko, A. A. Aravin, D. Esyunina, A. Kulbachinskiy, A programmable pAgo nuclease with universal guide and target specificity from the mesophilic bacterium Kurthia massiliensis. *Nucleic Acids Research*. **49**, 4054–4065 (2021).

19. K. S. Makarova, Y. I. Wolf, J. van der Oost, E. V. Koonin, Prokaryotic homologs of Argonaute proteins are predicted to function as key components of a novel system of defense against mobile genetic elements. *Biology Direct*. **4**, 29 (2009).

20. D. C. Swarts, J. J. Koehorst, E. R. Westra, P. J. Schaap, J. van der Oost, Effects of Argonaute on Gene Expression in Thermus thermophilus. *PLOS ONE*. **10**, e0124880 (2015).

21. A. Kuzmenko, A. Oguienko, D. Esyunina, D. Yudin, M. Petrova, A. Kudinova, O. Maslova, M. Ninova, S. Ryazansky, D. Leach, A. A. Aravin, A. Kulbachinskiy, DNA targeting and interference by a bacterial Argonaute nuclease. *Nature*. **587**, 632–637 (2020).

22. F. Jiang, J. A. Doudna, CRISPR–Cas9 Structures and Mechanisms. *Annual Review of Biophysics*. **46**, 505–529 (2017).

23. M. Christian, T. Cermak, E. L. Doyle, C. Schmidt, F. Zhang, A. Hummel, A. J. Bogdanove, D. F. Voytas, Targeting DNA Double-Strand Breaks with TAL Effector Nucleases. *Genetics*. **186**, 757–761 (2010).

24. J. C. Miller, S. Tan, G. Qiao, K. A. Barlow, J. Wang, D. F. Xia, X. Meng, D. E. Paschon, E. Leung, S. J. Hinkley, G. P. Dulay, K. L. Hua, I. Ankoudinova, G. J. Cost, F. D. Urnov, H. S. Zhang, M. C. Holmes, L. Zhang, P. D. Gregory, E. J. Rebar, A TALE nuclease architecture for efficient genome editing. *Nat Biotechnol*. **29**, 143–148 (2011).

25. F. D. Urnov, E. J. Rebar, M. C. Holmes, H. S. Zhang, P. D. Gregory, Genome editing with engineered zinc finger nucleases. *Nat Rev Genet*. **11**, 636–646 (2010).

26. D. Carroll, Progress and prospects: Zinc-finger nucleases as gene therapy agents. *Gene Ther*. **15**, 1463–1468 (2008).

27. M. S. Dillingham, S. C. Kowalczykowski, RecBCD Enzyme and the Repair of Double-Stranded DNA Breaks. *Microbiology and Molecular Biology Reviews*. **72**, 642–671 (2008).

28. A. K. Sinha, C. Possoz, D. R. F. Leach, The Roles of Bacterial DNA Double-Strand Break Repair Proteins in Chromosomal DNA Replication. *FEMS Microbiology Reviews*. **44**, 351–368 (2020).

29. J. K. Eykelenboom, J. K. Blackwood, E. Okely, D. R. F. Leach, SbcCD Causes a Double-Strand Break at a DNA Palindrome in the Escherichia coli Chromosome. *Molecular Cell*. **29**, 644–651 (2008).

30. G. R. Smith, How RecBCD Enzyme and Chi Promote DNA Break Repair and Recombination: a Molecular Biologist's View. *Microbiology and Molecular Biology Reviews*. **76**, 217–228 (2012).

31. D. B. Wigley, Bacterial DNA repair: recent insights into the mechanism of RecBCD, AddAB and AdnAB. *Nat Rev Microbiol*. **11**, 9–13 (2013).

32. B. M. Hall, C.-X. Ma, P. Liang, K. K. Singh, Fluctuation AnaLysis CalculatOR: a web tool for the determination of mutation rate using Luria–Delbrück fluctuation analysis. *Bioinformatics*. **25**, 1564–1565 (2009).

33. R. Vaiskunaite, J. Vainauskas, J. Morris, V. Potapov, J. Bitinaite, Programmable Cleavage of Double-stranded DNA by Combined Action of Argonaute CbAgo from Clostridium butyricum and Nuclease Deficient RecBC Helicase from E.coli (2021), p. 2021.07.01.450725, doi:10.1101/2021.07.01.450725.

34. J. M. Pennington, S. M. Rosenberg, Spontaneous DNA breakage in single living Escherichia coli cells. *Nat Genet*. **39**, 797–802 (2007).

35. R. J. Citorik, M. Mimee, T. K. Lu, Sequence-specific antimicrobials using efficiently delivered RNA-guided nucleases. *Nat Biotechnol*. **32**, 1141–1145 (2014).

36. A. F. Taylor, G. R. Smith, Substrate specificity of the DNA unwinding activity of the RecBC enzyme of Escherichia coli. *Journal of Molecular Biology*. **185**, 431–443 (1985).

37. F. N. Capaldo, S. D. Barbour, DNA content, synthesis and integrity in dividing and non-dividing cells of rec− strains of Escherichia coli K12. *Journal of Molecular Biology*. **91**, 53–66 (1975).

38. A. Kuzminov, F. W. Stahl, Stability of linear DNA in recA mutant Escherichia coli cells reflects ongoing chromosomal DNA degradation. *Journal of Bacteriology*. **179**, 880–888 (1997).

39. K. Skarstad, E. Boye, Degradation of individual chromosomes in recA mutants of Escherichia coli. *Journal of Bacteriology*. **175**, 5505–5509 (1993).

40. Deletions at stalled replication forks occur by two different pathways. *The EMBO Journal*. **16**, 3332–3340 (1997).

41. B. Michel, Replication fork arrest and DNA recombination. *Trends in Biochemical Sciences*. **25**, 173–178 (2000).

42. W. Jiang, D. Bikard, D. Cox, F. Zhang, L. A. Marraffini, RNA-guided editing of bacterial genomes using CRISPR-Cas systems. *Nat Biotechnol*. **31**, 233–239 (2013).

43. E. A. Moreb, B. Hoover, A. Yaseen, N. Valyasevi, Z. Roecker, R. Menacho-Melgar, M. D. Lynch, Managing the SOS Response for Enhanced CRISPR-Cas-Based Recombineering in E. coli through Transient Inhibition of Host RecA Activity. *ACS Synth. Biol.* **6**, 2209–2218 (2017).

44. K. Z. Lee, M. A. Mechikoff, A. Kikla, A. Liu, P. Pandolfi, K. Fitzgerald, F. S. Gimble, K. V. Solomon, NgAgo possesses guided DNA nicking activity. *Nucleic Acids Research*. **49**, 9926–9937 (2021).

45. I. Olovnikov, K. Chan, R. Sachidanandam, D. K. Newman, A. A. Aravin, Bacterial Argonaute Samples the Transcriptome to Identify Foreign DNA. *Molecular Cell*. **51**, 594–605 (2013).

46. L. Fu, C. Xie, Z. Jin, Z. Tu, L. Han, M. Jin, Y. Xiang, A. Zhang, The prokaryotic Argonaute proteins enhance homology sequence-directed recombination in bacteria. *Nucleic Acids Research*. **47**, 3568–3579 (2019).

47. S. M. Jolly, I. Gainetdinov, K. Jouravleva, H. Zhang, L. Strittmatter, S. M. Bailey, G. M. Hendricks, A. Dhabaria, B. Ueberheide, P. D. Zamore, Thermus thermophilus Argonaute Functions in the Completion of DNA Replication. *Cell*. **182**, 1545-1559.e18 (2020).

48. J. W. Hegge, D. C. Swarts, J. van der Oost, Prokaryotic Argonaute proteins: novel genome-editing tools? *Nat Rev Microbiol*. **16**, 5–11 (2018).

49. B. Enghiad, H. Zhao, Programmable DNA-Guided Artificial Restriction Enzymes. *ACS Synth. Biol.* **6**, 752–757 (2017).

50. A. Levy, M. G. Goren, I. Yosef, O. Auster, M. Manor, G. Amitai, R. Edgar, U. Qimron, R. Sorek, CRISPR adaptation biases explain preference for acquisition of foreign DNA. *Nature*. **520**, 505–510 (2015).

51. I. Ivančić-Baće, S. D. Cass, S. J. Wearne, E. L. Bolt, Different genome stability proteins underpin primed and naïve adaptation in E. coli CRISPR-Cas immunity. *Nucleic Acids Research*. **43**, 10821–10830 (2015).

52. J. W. Modell, W. Jiang, L. A. Marraffini, CRISPR–Cas systems exploit viral DNA injection to establish and maintain adaptive immunity. *Nature*. **544**, 101–104 (2017).

Acknowledgments:

We thank Dr. Alexei A. Aravin, Dr. Andrey Kulbachinskiy, Dr. Daria Esyunina, and Dr. David R. F. Leach for helpful discussions. We thank Rochelle A. Diamond and Jamie Tijerina for their help in flow cytometry experiments. All data necessary to support this paper's conclusions are available in the supplementary materials.

Author contributions:

S.H. designed and carried out experiments, with K.W. and S.L.M. providing guidance. S.H., K.W., and S.L.M. wrote the manuscript.

Conflict of interests:

The authors declare no competing financial interests.

SUPPLEMENTARY MATERIALS

Materials and Methods

Figures S1 to S4

Tables S1 to S7

References (*50-52)*

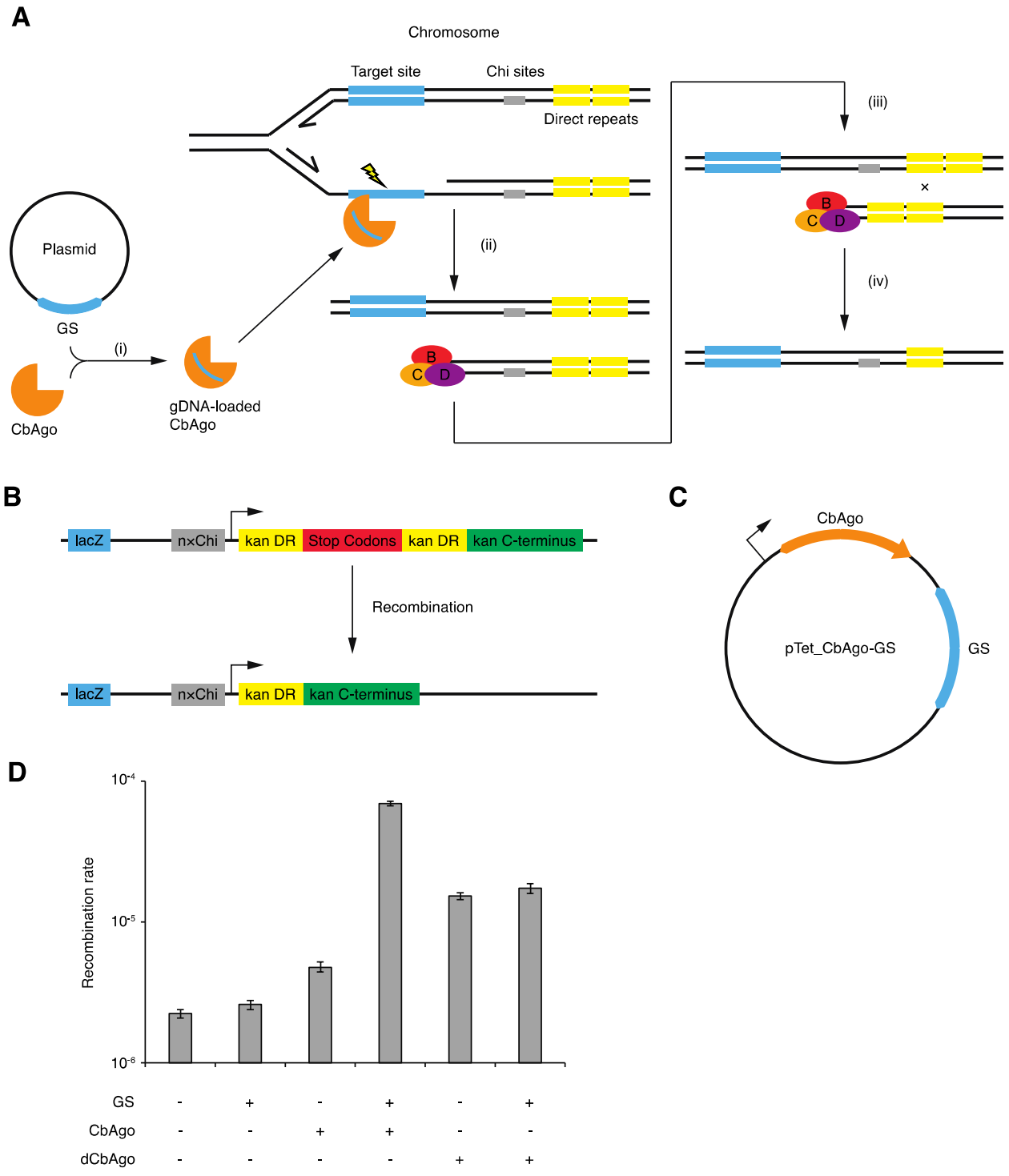

Fig .1. Guide-directed CbAgo cleavage stimulates chromosome recombination. (**A**) Proposed mechanism for guide-directed CbAgo cleavage and RecBCD-dependent recombination. (i) CbAgo acquires gDNA from plasmid-encoded GS. See fig. S1 for the

proposed model of gDNA biogenesis. (ii) Guide-directed CbAgo cleavage of lagging strand during chromosome replication generates DSB and (ii) triggers RecBCD binding and processing of chromosome DNA. (iii) Recognition of Chi sites by RecBCD attenuates its DNA degradation activity and facilitates recombination between sister chromosomes via RecA. (**B**) Structure of the recombination cassette. See supplementary materials and methods for DNA sequences. kan, kanamycin resistance gene. DR, direct repeat. (**C**) Structure of the CbAgo targeting plasmid. (**D**) Recombination rates of strain 3×ChikanS in different genetic contexts determined by fluctuation analysis from eight independent cultures. Error bars represent 95% confidence intervals.

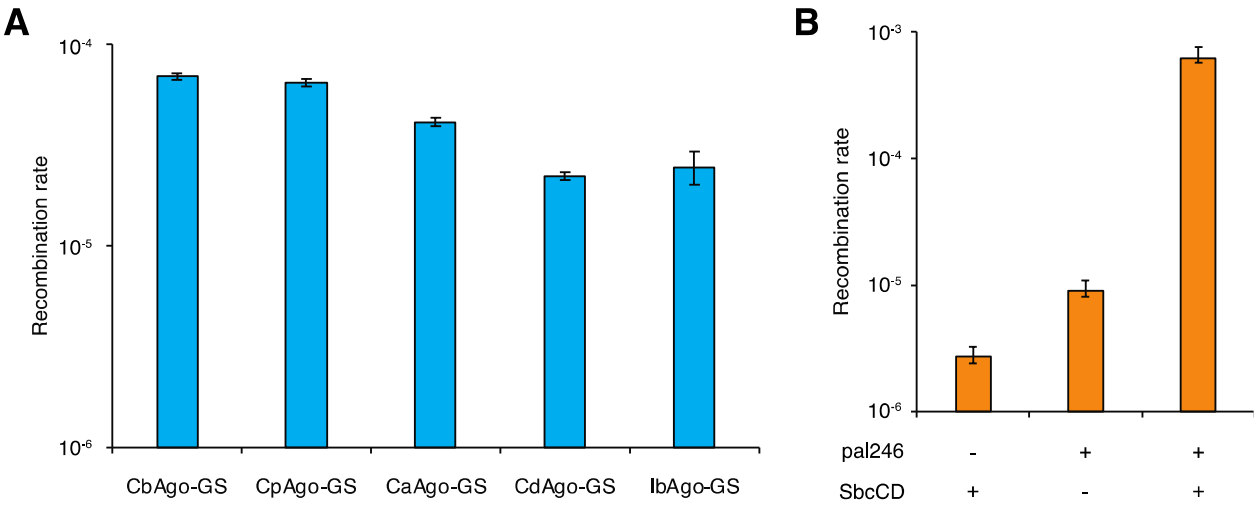

Fig. 2. Recombination rate by pAgo-GS correlates with pAgo *in vitro* DNA cleavage activity and *in vivo* DSB generation efficiency. (**A**) Recombination rates using different pAgos in the presence of GS in strain 3×ChikanS. See ref. *33* for comparisons of *in vitro* DNA cleavage activity among different pAgos. (**B**) Recombination rates using sbcCD^{+}/ΔsbcCD, lacZ^{+}/lacZ::pal246 strains. Strains used here were 3×ChikanS, 3×ChikanS_pal246_ΔsbcCD and 3×ChikanS_pal246. See ref. *21* for the comparison of *in vivo* DSB generation efficiency between SbcCD-pal246 and CbAgo-GS. See fig. S2 for the genetic structure of engineered DSB. Recombination rates were determined by fluctuation analysis from eight independent cultures. Error bars represent 95% confidence intervals.

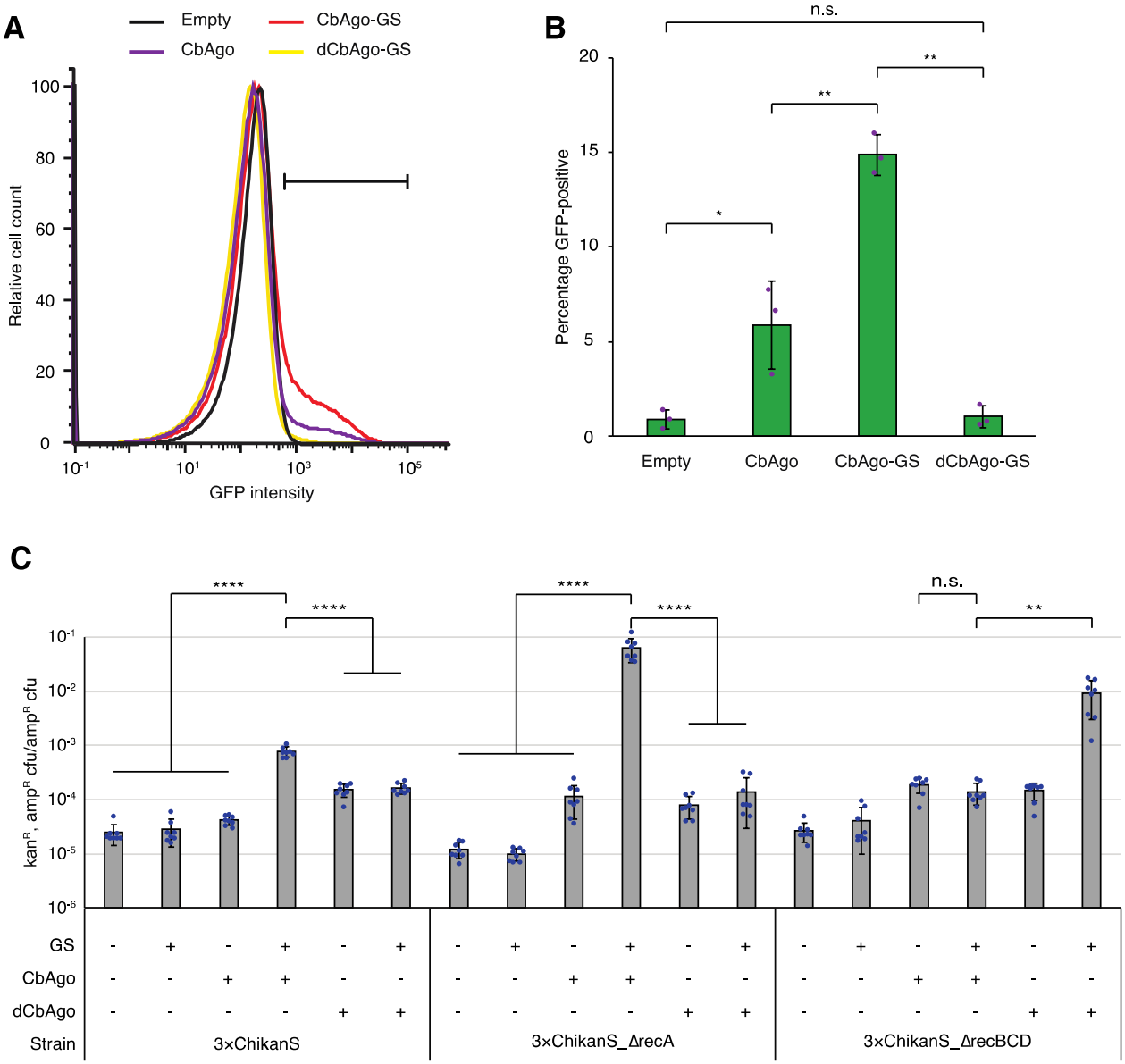

Fig. 3. Recombination by CbAgo-GS depends on DSB generation and RecBCD processing but is independent of RecA. (**A**) CbAgo-GS induces cellular SOS response. Flow cytometry histograms normalized to the mode of the population, combining data from three independent cultures. Horizontal bar represents the GFP^+ gate. (**B**) Quantification of GFP-positive cells within the GFP^+ gate. Error bars, mean ± s.d. from three independent cultures. (**C**) Recombination frequencies in different genetic contexts. Error bars, mean ± s.d. from eight independent cultures. n.s. $P > 0.05$, *$P < 0.05$, **$P < 0.01$, ***$P < 0.001$, ****$P < 0.0001$.

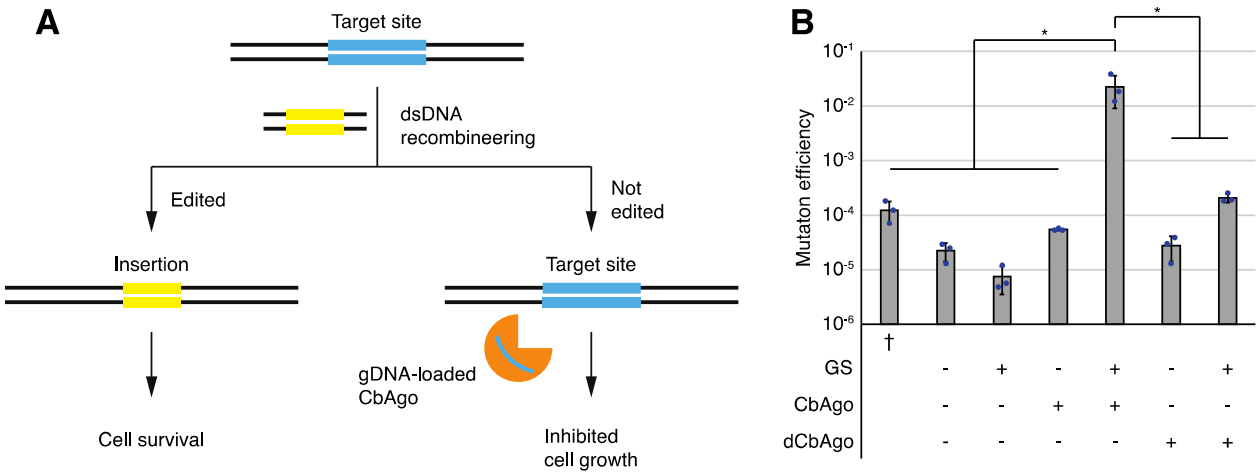

Fig. 4. Targeted CbAgo cleavage assists Lambda Red-mediated recombineering in RecA-deficient *E. coli* strain. (A) Scheme of CbAgo-assisted recombineering. After recombineering, the growth of unedited cells will be suppressed by CbAgo cleavage and subsequent DNA degradation, while successfully edited cells will be resistant to CbAgo cleavage and exhibit kanamycin resistance. Yellow, kanamycin resistance cassette. Blue, lacZ gene. (**B**) Mutation rates using strain SIJ488_ΔrecA in different genetic contexts. †Standard recombineering procedure was applied using plasmid-free cells. See supplementary materials and methods for details. Error bars, mean ± s.d. from three independent experiments. *P < 0.05.